

Original investigation

Functional Connectivity During Exposure to Favorite-Food, Stress, and Neutral-Relaxing Imagery Differs Between Smokers and Nonsmokers

Kathleen A. Garrison PhD¹, Rajita Sinha PhD², Cheryl M. Lacadie BS³,
Dustin Scheinost PhD³, Ania M. Jastreboff MD, PhD⁴, R. Todd Constable PhD³,
Marc N. Potenza MD, PhD⁵

¹Department of Psychiatry, Yale School of Medicine, New Haven, CT; ²Department of Psychiatry, Child Study Center, and Neurobiology, Yale School of Medicine, New Haven, CT; ³Department of Diagnostic Radiology, Yale School of Medicine, New Haven, CT; ⁴Department of Internal Medicine, Division of Endocrinology, and Department of Pediatrics, Division of Pediatric Endocrinology, Yale School of Medicine, New Haven, CT; ⁵Department of Psychiatry and Child Study Center, Neurobiology, and CASA Columbia, Yale School of Medicine, and Connecticut Mental Health Center, New Haven, CT

Corresponding Author: Kathleen A. Garrison, PhD, Department of Psychiatry, Yale School of Medicine, 1 Church Street #730, New Haven, CT 06511, USA. Telephone: 203-737-6232, Fax: 203-737-3591; E-mail: kathleen.garrison@yale.edu

Abstract

Introduction: Tobacco-use disorder is a complex condition involving multiple brain networks and presenting with multiple behavioral correlates including changes in diet and stress. In a previous functional magnetic resonance imaging (fMRI) study of neural responses to favorite-food, stress, and neutral-relaxing imagery, smokers versus nonsmokers demonstrated blunted corticostriatal-limbic responses to favorite-food cues. Based on other recent reports of alterations in functional brain networks in smokers, the current study examined functional connectivity during exposure to favorite-food, stress, and neutral-relaxing imagery in smokers and nonsmokers, using the same dataset.

Methods: The intrinsic connectivity distribution was measured to identify brain regions that differed in degree of functional connectivity between groups during each imagery condition. Resulting clusters were evaluated for seed-to-voxel connectivity to identify the specific connections that differed between groups during each imagery condition.

Results: During exposure to favorite-food imagery, smokers versus nonsmokers showed lower connectivity in the supramarginal gyrus, and differences in connectivity between the supramarginal gyrus and the corticostriatal-limbic system. During exposure to neutral-relaxing imagery, smokers versus nonsmokers showed greater connectivity in the precuneus, and greater connectivity between the precuneus and the posterior insula and rolandic operculum. During exposure to stress imagery, smokers versus nonsmokers showed lower connectivity in the cerebellum.

Conclusions: These findings provide data-driven insights into smoking-related alterations in brain functional connectivity patterns related to appetitive, relaxing, and stressful states.

Implications: This study uses a data-driven approach to demonstrate that smokers and nonsmokers show differential patterns of functional connectivity during guided imagery related to personalized favorite-food, stress, and neutral-relaxing cues, in brain regions implicated in attention, reward-related, emotional, and motivational processes. For smokers, these differences in connectivity may impact appetite, stress, and relaxation, and may interfere with smoking cessation.

Introduction

Most current adult cigarette smokers want to quit, and nearly half attempt quitting annually¹; however, most relapse to smoking due to withdrawal symptoms, stress, and weight gain.² A better understanding of disruptions in cognition, affect, and motivation associated with smoking may improve smoking cessation treatments. Functional magnetic resonance imaging (fMRI) has been used to evaluate brain activity related to cognitive, emotional and motivational tasks in smokers. Such task activation-based studies have suggested differences between smokers and nonsmokers including increased activity in reward-related brain regions in response to smoking cues,³ as well as differences in brain activity in response to food cues^{4,5} and stress cues.^{6,7} fMRI has also been used to evaluate brain functional connectivity in smokers during task performance or at rest.⁸ These studies have demonstrated differences between smokers and nonsmokers in large-scale brain network dynamics in the resting-state and related to cognitive processes such as craving.⁹ Functional connectivity studies provide additional insights into systems-level changes in the brain associated with smoking, potentially leading to new hypotheses about the neurobiological underpinnings of tobacco-use disorder.¹⁰

Based on evidence that functional connectivity analysis can complement and extend task activation-based analysis in studies of smoking, the current study sought to evaluate functional connectivity in smokers using the same dataset from a previously published task activation-based study.¹¹ Functional connectivity was compared between smokers and nonsmokers during exposure to personalized guided favorite-food, stress, and neutral-relaxing imagery. This guided imagery task has been used previously to evaluate stress and craving related to addictions,^{12,13} including nicotine dependence^{14,15} and obesity,¹⁶ as well as other psychiatric disorders.¹⁷ In the earlier task activation-based analysis of this dataset, smokers versus nonsmokers were found to have blunted corticostriatal-limbic responses to favorite-food imagery, and no group differences were found in task activations during stress or neutral-relaxing imagery.¹¹

The current study used a relatively new approach to identify group differences in functional connectivity for each imagery condition: the intrinsic connectivity distribution (ICD¹⁸). In contrast to seed-based connectivity methods which require a priori regions of interest, ICD is a data-driven measure of connectivity between each voxel and every other voxel in the brain. As a data-driven approach, ICD permits both the independent support of established hypotheses—here, that smokers will show differences in functional connectivity in motivation-reward brain regions during favorite-food imagery—and the discovery of novel patterns of functional connectivity that may be missed by hypothesis-driven approaches. Other studies have used independent components analysis (ICA¹⁹) to compare functional connectivity between smokers and nonsmokers^{20,21} or other related to other addictions.^{22,23} In contrast to group ICA which estimates a common set of components or networks for a group, ICD does not assign voxels to particular components, and may therefore provide a complementary picture of differences in functional connectivity between smokers and nonsmokers.

Although these methods are typically applied to resting-state fMRI data, the current guided imagery task resulted in a large amount of continuous task data that approximates the conditions of resting-state data with no task boundaries. We have used similar approaches to study meditation with ICD²⁴ and seed-based functional connectivity.^{24,25} We have also performed ICD on functional Stroop data in cocaine-dependent and healthy comparison subjects.²⁶

Further emerging research suggests that resting-state fMRI methods are suitable in the context of task fMRI.^{27,28}

ICD was first used to identify brain regions that differ in connectivity between groups for each imagery condition. Resulting clusters were then tested for seed-to-voxel connectivity to identify which specific connections with these brain regions differed between groups for each imagery condition.

Methods

Participants

Twenty-three smokers (mean age 27 ± 7 years, 10 females) and 23 nonsmokers (mean age 27 ± 7 years, nine females) participated in the study (Table 1). Daily smokers who smoked ≥ 10 cigarettes per day were recruited for the study.¹¹ However, smokers had low nicotine dependence as indicated by low scores (mean 2.5 ± 2.0) on the Fagerström Test for Nicotine Dependence.²⁹ At the time of scanning, several smokers had reduced their smoking frequency to less than 10 cigarettes per day (mean 9.4 ± 7.1 , range 0.27–28 cigarettes per day at time of scanning), as measured using the Time line Follow back³⁰ for the past 30 days. Smoking characteristics assessed included the number of cigarettes smoked per day, age at onset of smoking, years to smoking, carbon monoxide level, and Fagerström Test for Nicotine Dependence. Smokers carbon monoxide levels also indicated a light to moderate smoking range (mean 12.5 ± 9.3 parts per million). Nonsmokers were required to have no tobacco consumption for more than 1 year and have never used tobacco daily. Smokers and nonsmokers were matched on age, gender, intelligence quotient, and body mass index. Participants were additionally required to be age 18–50 years old and able to read and write English. Exclusion criteria included any chronic medical condition, neurological injury or illness, psychiatric disorder (*DSM-IV* criteria), or substance-use disorder (other than nicotine dependence); use of any psychoactive medication within the past 4 weeks; any chronic medication use for medical problems or psychiatric disorders; any alcohol or drug use in the past 72 hours prior to scanning (other than tobacco); intelligence quotient < 90; and pregnancy, claustrophobia, or metal in body incompatible with MRI. The study was approved by the Yale Human Investigation Committee. All participants provided signed informed consent.

Table 1. Participant Demographics

	Smokers (N = 23)	Nonsmokers (N = 23)
	Mean ± SD	Mean ± SD
Demographics		
Age (y)	26.7 ± 7.1	27.4 ± 7.3
Gender (female)	43%	39%
IQ	112.1 ± 8.6	112.6 ± 9.6
BMI (kg/m ²)	28.0 ± 4.6	26.8 ± 5.1
Smoking measures		
Cigarettes per day	9.4 ± 7.1	0
FTND score	2.5 ± 2.0	0
CO levels	12.5 ± 9.3	2.4 ± 1.0*
Years smoked	7.5 ± 9.0	0
Age at onset of smoking	18.2 ± 2.5	0

BMI = body mass index; CO = carbon monoxide, in parts per million; FTND = Fagerström test for nicotine dependence; IQ = intelligence quotient.

* $P < .0001$.¹¹

Imagery Script Development

Prior to a participant's fMRI session, personalized guided imagery scripts were generated using scene construction questionnaires (as in Sinha³¹). Two favorite-food scripts were developed from participants' descriptions of two of their favorite foods, such as cheese-cake, ice cream, or pizza, and events associated with these foods. Two neutral-relaxing scripts were developed from participants' personal experiences of common neutral-relaxing situations, such as a summer day relaxing at the beach or a fall day reading in the park. Two stress scripts were developed from participants' descriptions of two recent (past year) personal stressful events that were rated as 8 or above on a 10-point Likert scale from "1 = not at all stressful" to "10 = most stress you felt recently in your life," such as a breakup with a significant other, unemployment, or death of a loved one. Smoking-related experiences were excluded from consideration. For example scripts see.^{16,32} For each condition, two scripts, 2 minutes in length each, were developed and audio-recorded, to be presented during fMRI. Participants were trained to generate and maintain a mental image for 2–3 minutes and were trained in progressive relaxation to employ prior to fMRI and between imagery conditions.

Imaging Sessions

fMRI sessions took place in the early afternoon. All participants were instructed to eat approximately 2 hours beforehand to avoid being too hungry or too full. Smokers were instructed to smoke approximately 1 hour beforehand to avoid acute intoxication or withdrawal. During fMRI, participants were exposed to personalized favorite-food, stress, and neutral-relaxing imagery conditions. The fMRI session included six trials, two per condition, randomized and counterbalanced. Each trial included a 1.5-minute resting baseline, followed by a 2.5-minute guided imagery period and 1-minute quiet recovery period. During the 2.5-minute guided imagery period, participants were instructed via headphones to "close your eyes and imagine the situation being described as if it were happening right now." A previously audiotaped 2-minute description of their personal appetitive, stressful, or neutral-relaxing event was then presented, followed by 0.5 minutes of quiet imagery time during which they continued imagining the story while lying in silence. At the end of the guided imagery period, participants were asked to "stop imagining and lay still" and scanning continued through the next 1-minute quiet recovery period. Participants next rated their imagery vividness, subjective anxiety and tobacco craving levels on an analog scale from 0 to 10 with 0 = none, 1–3 = mild, 4–7 = moderate and 8–10 = intense feelings. After each trial, participants listened to progressive relaxation instructions during a 5-minute rest/recovery period.

Task Validation

Task validation was reported previously¹¹ based on subjective ratings for anxiety and food cravings before and after each imagery condition, and imagery vividness ratings, which were comparable between smokers and nonsmokers. In addition, for smokers, baseline tobacco craving ratings did not differ between imagery conditions ($F(2) = 0.25$, $P = .77$), and tobacco craving ratings increased after favorite-food imagery ($P = .0001$) and after stress imagery ($P = .006$), and decreased after neutral-relaxing imagery ($P = .029$).

Image Acquisition

Brain images were acquired using a 3 Tesla Siemens Trio MRI scanner and standard-quadrature head coil at the Yale Magnetic Resonance Research Center. A T1 Fast Low Angle Shot imaging

sequence was acquired in the axial plane parallel to the anterior-posterior commissure (AC-PC) line (repetition time [TR] = 300 ms, echo time [TE] = 2.46 ms, bandwidth = 310 Hz/pixel, flip angle = 60°, field-of-view = 220×220 mm, matrix = 256×256, 32 slices, slice thickness = 4 mm, no gap). A T2*-weighted gradient-recalled single-shot echo-planar pulse imaging sequence was acquired with 32 axial slices parallel to the AC-PC line covering the whole brain (TR = 2000 ms, TE = 25 ms, bandwidth = 2005 Hz/pixel, flip angle = 85°, field-of-view = 220×220 mm, matrix = 64×64, 32 slices, slice thickness = 4 mm, no gap, 150 measurements). A high-resolution 3D Magnetization-Prepared Rapid Gradient-Echo sequence was then acquired in the sagittal plane for multi-subject registration (TR = 2530 ms; TE = 3.34 ms; bandwidth = 180 Hz/pixel; flip angle = 7°; slice thickness = 1 mm; field-of-view = 256×256 mm; matrix = 256×256).

Image Quality Assessment and Attrition

Two smokers' datasets were excluded from the final analysis as they showed less than 2 SDs of the mean global signal change during imagery and no activation of the auditory cortex. Data are therefore reported from 21 smokers and 23 nonsmokers.¹¹

fMRI Preprocessing

The first 10 images were discarded to enable the signal to achieve steady-state. Images were motion corrected using SPM5 (www.fil.ion.ucl.ac.uk/spm). Images were iteratively smoothed until the smoothness for any image had a full width half maximum of approximately 6 mm.³³ This iterative smoothing has been shown to minimize motion confounds associated with functional connectivity.³⁴ All further analysis was performed using BioImage Suite (www.bioimagesuite.org).³⁵ Several covariates of no interest were regressed from the data including linear and quadratic drift, six rigid-body motion parameters, mean cerebrospinal fluid signal, mean white-matter signal, and overall global signal. All images were temporally smoothed using a zero mean unit Gaussian filter with an approximate cutoff of 0.12 Hz. A canonical gray-matter mask, defined on the Montreal Neurological Institute (MNI) template brain and dilated to ensure that all gray matter was captured on the low-resolution fMRI images, was applied to restrict the analysis to gray-matter voxels.

ICD Analysis

After preprocessing, the two runs for each imagery condition were concatenated and functional connectivity at each voxel was calculated in each participant's individual space as the ICD.¹⁸ Only the imagery periods were used for ICD analysis; both the baseline and recovery periods were excluded. The ICD approach computes the correlation between the time course at a given voxel in the gray matter and the time courses of every other voxel in the gray matter, and summarizes these using a network theory metric, degree. ICD models the entire distribution of the network measure of degree, eliminating the need to specify a connection threshold. Only positive correlations were tested because the global signal regression (GSR) employed in preprocessing results in ambiguous directions of correlations. A histogram of the positive correlations is constructed to estimate the distribution of connections to a given voxel (using a threshold of 0.0001 for numerical stability), and the histogram is converted into a survival function fitted with a stretched exponential with unknown variance, α . This is repeated for each gray matter voxel, resulting in a parametric map of α for each participant, where each voxel in the map represents that voxel's correlation to the rest

of the gray matter. In order to further evaluate relative differences in ICD, each participant's α map was mean-adjusted to the whole-brain α by subtracting the mean and dividing by the SD across all voxels. This z -score-like normalization adjusts for large differences in global connectivity between participants.²⁶ Next, individual ICD maps were warped to MNI space using a series of linear and nonlinear transformations (as in Scheinost et al³⁶). Voxel-wise two-sample t tests were used to compare ICD between smokers and nonsmokers during each imagery condition. Findings are reported at $P < .05$ Family Wise Error cluster-corrected, with cluster size determined using AlphaSim (<http://afni.nimh.nih.gov>) for gray matter and Bonferroni-corrected for three t tests, $k = 172$ (such that significance for each independent comparison was $P < .0167$ at the cluster-level).

Notably, GSR can possibly induce some negative relationships,³⁷ thus complicating interpretation. However, GSR is widely used in the literature and by other groups conducting similar voxel-to-voxel correlation approaches.³⁸⁻⁴² Additionally, in a large sample of healthy adults, ICD results with and without GSR were nearly identical.³⁶ Due to the controversy of using GSR,⁴³⁻⁴⁵ the ICD analyses were repeated without removing the global signal, and the results are largely the same (see [Supplementary Material](#)), suggesting the robustness of our findings to this preprocessing choice.

Seed-to-Voxel Connectivity Analysis

Secondary seed-to-voxel connectivity analysis was performed to explore (post hoc) regions of interest identified by ICD analysis. ICD and similar voxel-to-voxel correlation approaches compress all connectivity information about a voxel into a single number. As such, any spatial information about which connections are responsible for the change in connectivity to that voxel is lost. Post hoc discovery of these specific connections was explored with follow-up seed-to-voxel connectivity. Resulting significant clusters from between-group ICD comparisons were masked and used as seeds. The time course of the seed in a given participant was computed as the average time course across all voxels in the seed. This time course was correlated with the time course for every other voxel in the brain to create a map of r -values, reflecting seed-to-whole brain connectivity. These r -values were transformed to z -values using Fisher's transform, yielding one map for each participant representing the strength of the correlation to the seed. Voxel-wise two-sample t tests were used to compare seed-to-voxel connectivity between smokers and nonsmokers during each imagery condition. Findings are reported at $P < .05$ Family Wise Error cluster-corrected, $k = 147$.

Motion Comparison

Finally, although motion parameters were regressed from the data, group differences in movement may influence functional connectivity measures. To test this, the average frame-to-frame displacement was calculated for each participant for each imagery condition, and compared using a mixed 2×3 (group \times imagery condition) analysis of variance. No significant effect was found for imagery condition ($F = 1.9$, $P = .15$) or group ($F = 1.1$, $P = .3$), and no significant interaction was found ($F = 0.54$, $P = .58$). Additionally, we used an iterative smoothing algorithm which been shown to minimize these motion confounds.³⁴

Results

Functional Connectivity During Exposure to Favorite-Food Imagery

Smokers compared to nonsmokers showed lower ICD during exposure to favorite-food imagery in the bilateral supramarginal gyrus, extending into the postcentral gyrus and inferior parietal lobule, both with mean adjustment ([Figure 1A](#)) and without mean adjustment (not shown). These clusters were used as seeds to test for seed-to-voxel connectivity. For the left supramarginal gyrus, smokers showed greater connectivity than nonsmokers with the left inferior frontal gyrus, putamen, and pallidum, bilateral superior medial frontal gyrus into the middle cingulate gyrus, and the hippocampus and brainstem, and less connectivity with the left precentral gyrus, bilateral postcentral gyrus, supramarginal gyrus and precuneus, and the occipital gyrus ([Figure 1B](#)). For the right supramarginal gyrus, smokers showed greater connectivity than nonsmokers with the left precentral gyrus, inferior frontal gyrus, superior medial frontal gyrus into the middle cingulate gyrus, and pallidum, bilateral putamen and thalamus, right basal forebrain and amygdala, and the posterior cingulate cortex, and less connectivity with the left postcentral gyrus and occipital gyrus ([Figure 1C](#)).

Functional Connectivity During Exposure to Neutral-Relaxing Imagery

Smokers compared to nonsmokers showed greater mean-adjusted ICD in the precuneus during exposure to neutral-relaxing imagery ([Figure 2A](#)). No group differences were found without mean adjustment. The cluster in the precuneus was used as a seed to test for seed-to-voxel connectivity. Smokers compared to nonsmokers showed greater connectivity between the precuneus and the posterior insula, rolandic operculum and Heschl's gyrus, and the precuneus/cuneus, and lower connectivity between the precuneus and the cerebellum ([Figure 2B](#)).

Functional Connectivity During Exposure to Stress Imagery

Smokers compared to nonsmokers showed lower ICD in the cerebellum during exposure to stress imagery, both with mean adjustment ([Figure 3](#)) and without mean adjustment (not shown). No brain regions showed a significant group difference in seed-to-voxel connectivity from this cluster.

Discussion

These analyses demonstrate that smokers and nonsmokers show differential patterns of functional connectivity during guided imagery related to personalized favorite-food, stress, and neutral-relaxing cues, as evaluated using ICD and seed-to-voxel connectivity analyses. Specific findings vary by imagery condition and are discussed below. Overall, smokers and nonsmokers show differences in ICD and seed-to-voxel connectivity in brain regions implicated in attention, reward, and emotional or motivational processing, related to appetitive, stressful, and relaxing states.

Circuit-level interactions between brain regions have previously been found to differ between smokers and nonsmokers. These studies typically evaluate functional connectivity of resting-state fMRI data, either by measuring seed-based connectivity from specific brain regions of interest⁴⁶ or by using ICA to estimate a common

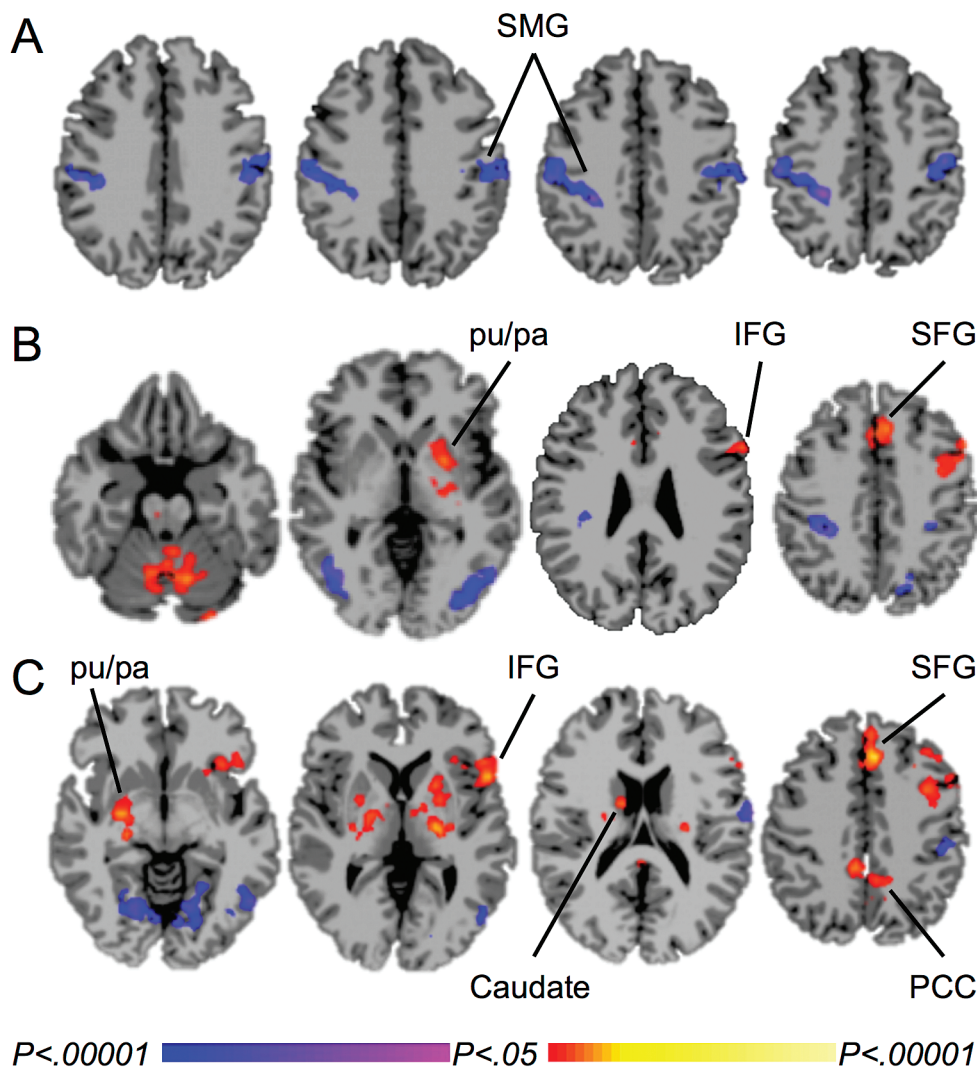


Figure 1. Differences in functional connectivity between smokers and nonsmokers during exposure to favorite-food imagery. **A.** Lower mean-adjusted intrinsic connectivity distribution (ICD) in smokers than nonsmokers in the supramarginal gyrus. **B.** Between-group differences in functional connectivity from the left supramarginal gyrus. **C.** Between-group differences in functional connectivity from the right supramarginal gyrus. Warm colors represent areas with greater connectivity for smokers than nonsmokers; cool colors represent areas with greater connectivity for nonsmokers than smokers. $P_{FWE} < .05$. SMG = supramarginal gyrus, pu = putamen, pa = pallidum, IFG = inferior frontal gyrus, SFG = superior medial frontal gyrus, PCC = posterior cingulate cortex.

set of components or networks to compare between groups,⁴⁷⁻⁴⁹ or using both approaches.⁵⁰ Similar to the ICA approach, ICD is a data-driven voxel-wise measure of intrinsic functional connectivity that does not rely on a priori regions of interest. In contrast to ICA, ICD does not constrain voxels to networks and may therefore be more sensitive to group differences.³⁶ The current study also evaluated ICD during a cognitive task paradigm rather than at rest, in order to compare functional connectivity between smokers and nonsmokers related to cognitive processing for task demands. The imagery task used in this study resulted in a large amount of continuous data (two 2.5-minute runs, concatenated) able to be analyzed using this approach. First, ICD was measured to identify regions of the brain that differed in the degree of connectivity between smokers and nonsmokers during each condition of the personalized guided imagery task. Next, seed-to-voxel connectivity was evaluated to determine which specific connections from these identified brain regions differed between smokers and nonsmokers during each

imagery condition. Our findings complement other recent studies reporting differences in functional connectivity between smokers and nonsmokers.

Group Differences in Visuomotor and Motivation/Reward Processing During Exposure to Favorite-Food Imagery

During exposure to favorite-food imagery, smokers showed lower ICD than nonsmokers in the bilateral supramarginal gyrus. The supramarginal gyrus and inferior parietal lobule have been reported in fMRI studies of the neural responses to food-cues versus non-food-cues.⁵¹⁻⁵³ A recent fMRI study of the cognitive regulation of food craving in adolescents (mean age 15 years) found that imagining eating as compared to thinking about the costs of eating in response to food-cues engaged the left supramarginal gyrus.⁵⁴ The supramarginal gyrus, along with the precuneus and superior parietal lobule, have also been reported in fMRI studies of smoking-related cues

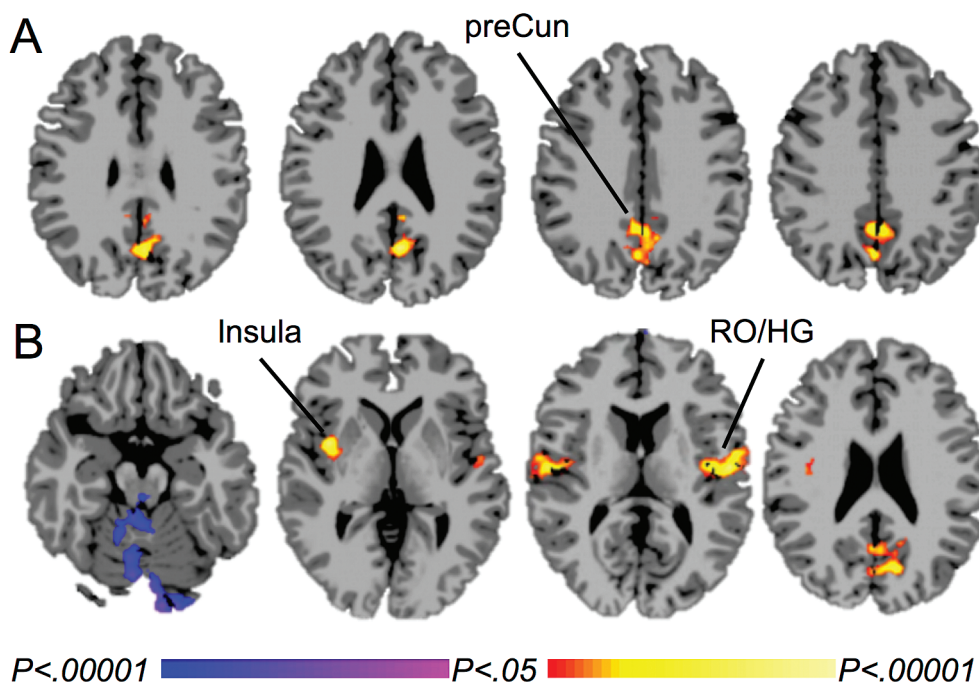


Figure 2. Differences in functional connectivity between smokers and nonsmokers during exposure to neutral-relaxing imagery. **A.** Greater mean-adjusted intrinsic connectivity distribution (ICD) in smokers than nonsmokers in the precuneus. **B.** Between-group differences in functional connectivity from the precuneus. Warm colors represent areas with greater connectivity for smokers than nonsmokers; cool colors represent areas with greater connectivity for nonsmokers than smokers. $P\text{-FWE} < .05$. preCun = precuneus, RO = rolandic operculum, HG = Heschl's gyrus.

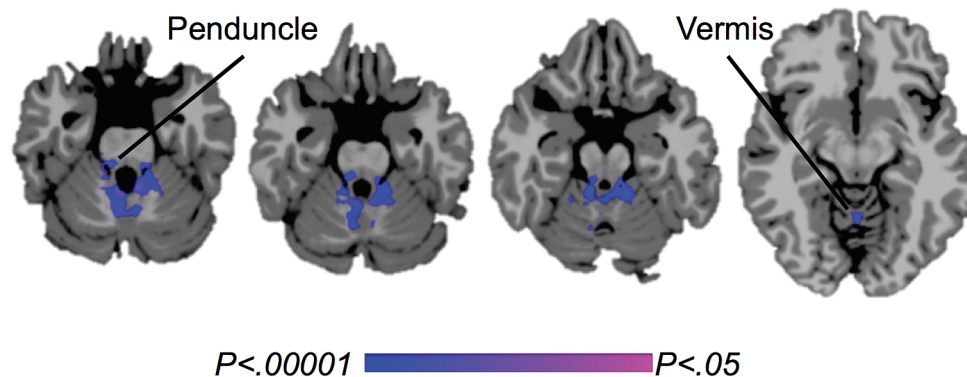


Figure 3. Differences in functional connectivity between smokers and nonsmokers during exposure to stress imagery. Lower mean-adjusted intrinsic connectivity distribution (ICD) in smokers versus nonsmokers in the cerebellar peduncles and vermis (cool colors). $P\text{-FWE} < .05$.

versus nonsmoking-related cues.³ For example, one study found the supramarginal gyrus along with other brain regions to be activated in response to smoking-related cues and positively correlated with craving.⁵⁵ Activation of visuomotor brain regions such as the supramarginal gyrus in response to food- and smoking-related cues might reflect visual processing, imagery, and/or preparation of approach-related actions toward food- or smoking-related stimuli. Consistent with the role of the supramarginal gyrus in imagery, this brain region has been found to be activated in response to “enacted memories.”⁵⁶ In that study, subjects encoded action phrases such as “cut the bread” either by reading them aloud or by enacting them. When presented with the phrases during fMRI, the bilateral supramarginal gyrus was more strongly engaged by previously enacted versus verbally encoded phrases. Overall, lower ICD in the supramarginal gyrus during exposure to favorite-food imagery in smokers versus nonsmokers may reflect reduced visuomotor processing or imagery.

The earlier task activation-based analysis of this dataset¹¹ revealed reduced corticostriatal-limbic responses to favorite-food cues in smokers compared to nonsmokers, including reduced activations in the caudate, putamen, insula, thalamus, and brainstem. In the current analysis, smokers compared to nonsmokers showed greater connectivity during favorite-food imagery between the supramarginal gyrus and similar brain regions including the putamen, pallidum, thalamus, basal forebrain and amygdala, hippocampus, and brainstem. Together these analyses show correlated reduced activity in motivation-reward brain regions/circuits during favorite-food imagery in smokers, suggesting that smokers may be desensitized to food-related rewards, although additional studies should further investigate this interpretation. This is consistent with evidence that brain reward circuits in drug-addicted individuals are desensitized to natural rewards and motivational salience for nondrug-related stimuli is decreased.⁵⁷ Here smokers and nonsmokers were matched on body mass index,

suggesting that smokers show a blunted response to food-related rewards irrespective of body weight, which might contribute to a lower body weight in smokers⁵⁸ alongside the acute effects of nicotine to decrease appetite and reduce neural food cue-reactivity.^{59,60} Further, as reported previously,¹¹ smokers and nonsmokers did not differ in food craving in response to favorite-food imagery ($P = .69$), suggesting that group differences in reward processing may be subconscious. This is similar to an earlier study using the same guided imagery task,¹⁶ in which obese versus lean individuals showed greater activity in corticostriatal-limbic regions during exposure to favorite-food imagery despite no group differences in food craving. Group differences in response to favorite-food imagery are not found in craving ratings, but instead in brain reward-processing. A future study could test the relationship between this blunted response to food-related rewards, body mass index, and other eating habits, in smokers with a wider range of body mass index. Additionally, based on evidence that smoking cessation is associated with weight gain,⁵⁸ a future study could test whether this blunted response “recovers” with smoking cessation and this correlates with weight gain.

Group Differences in Precuneus Connectivity During Exposure to Neutral-Relaxing Imagery

During exposure to neutral-relaxing imagery, smokers showed greater ICD than nonsmokers in the precuneus, and greater connectivity between the precuneus and the posterior insula and rolandic operculum. The precuneus is implicated in a wide range of cognitive processes including visuospatial imagery, episodic and autobiographical memory, and self-related processing.⁶¹ The identified cluster is located in the ventral precuneus, considered a functional hub of the default mode network (DMN),^{62,63} brain regions activated during resting-state and deactivated during task-engagement and therefore implicated in mind-wandering and rumination.^{64,65} A recent neuroimaging meta-analysis found the precuneus, along with all DMN hubs and other non-DMN brain regions, to be reliably activated by mind-wandering and spontaneous thought processes.⁶⁶ Moreover, in a recent resting-state functional connectivity study, smokers showed diminished disengagement from DMN processing during short-term abstinence from smoking, resulting in alterations in large-scale resting-state network dynamics that were associated with craving and cognitive impairments, and may therefore interfere with smoking cessation.⁹ It is possible that greater ICD in the precuneus during neutral-relaxing imagery in smokers versus nonsmokers represents greater DMN processing. Together, these studies suggest that training smokers to disengage from DMN processing, for example through mindfulness-based interventions, may benefit smoking cessation.^{25,67,68}

The precuneus is also consistently reported in neuroimaging studies of smoking cue reactivity.³ A recent study found that short-term abstinent smokers showed greater functional connectivity in response to smoking versus neutral cues between an a priori seed in the anterior insula and the precuneus, that was correlated with smoking cue-induced craving.⁶⁹ It has been hypothesized that co-activations in the precuneus and anterior insula represent a salient interoceptive state elicited by smoking cues that draws resources away from executive control processes toward DMN processes.^{9,10} However, it is unlikely that greater precuneus connectivity in smokers during neutral-relaxing imagery reflects smoking cue-reactivity or craving, because personalized script development excluded smoking cues, smokers reported decreased craving across the neutral-relaxing imagery condition, and no differences in connectivity with the anterior insula were observed.

Group Differences in Cerebellar Connectivity During Exposure to Stress Imagery

During exposure to stress imagery, smokers showed lower ICD than nonsmokers in the cerebellum. Activation was localized to the cerebellar peduncles and vermis. There is evidence that the cerebellar vermis is a target of limbic connections to the cerebellum, and mid-line cerebellar structures have been implicated in the modulation of emotion and in neuropsychiatric impairments.⁷⁰ It is possible that lower functional connectivity in this region during stress exposure in smokers versus nonsmokers may contribute to alterations in emotional regulation or stress-responsiveness; however, this possibility warrants direct examination. More generally, the cerebellum has been implicated in brain processes in addiction such as reward, motivational drive, saliency, inhibitory control, and insight,^{71,72} although the role of the cerebellum in addiction has been understudied and further work is needed to directly assess its relevance.⁷¹

Limitations

A limitation of the current study was that the fMRI task did not include a smoking cue imagery condition. However, many studies have evaluated smoking cue-related brain activity³ and functional connectivity⁷³ in smokers. A future study might build on the current findings by testing personalized smoking imagery, based on other reports that personalization enhances behavioral⁷⁴ and neural⁷⁵ responses to smoking cues. Another limitation was the relatively low nicotine dependence of the smokers in this study, as evident by low Fagerström Test for Nicotine Dependence scores (mean 2.5 ± 2.0) and late onsets of smoking (mean 18.2 ± 2.5 years). Moreover, several participants reduced their smoking from the inclusion criteria (≥ 10 cigarettes/d) to light and intermittent smoking (range 0.27–28 cigarettes per day) by the day of scanning. To address this limitation, the ICD analyses were repeated including only daily smokers with a range of 4.67–28 cigarettes/d ($n = 18$), and the results are largely the same (see [Supplementary Material](#)). In addition, we extracted the ICD values for all smokers from the same masks used as seeds for the seed-to-voxel connectivity analyses (ie, the resulting significant clusters from the between-group ICD comparisons with nonsmokers) for each imagery condition, and tested for correlations with Fagerström Test for Nicotine Dependence and cigarettes per day. No significant correlations were identified. These findings are in line with other recent work showing tobacco-related effects in light smokers (tobacco “chippers”),^{76,77} including studies showing increased responses to cigarette cues and decreased responses to food cues in light smokers.^{78,79} More work is needed in larger samples to directly test for differences related to smoking severity. Another limitation of the present study is that, while we have been cautious in interpreting our findings, the cognitive processes implicated have been reasoned backward from brain activation patterns; that is, using reverse inference.⁸⁰ Our interpretations are constrained by the task setting (personalized favorite-food, stress, or neutral-relaxing imagery) which has been argued to improve the precision of reverse inference.^{80,81} Nevertheless, further work is needed to obtain a more complete picture of how cognitive processes related to these tasks differ between smokers and nonsmokers. In addition, as the current study tested post hoc seed-to-voxel connectivity to identify the specific connections responsible for overall group differences in ICD, the evaluation of an independent dataset is needed to confirm these findings. Finally, as mentioned above, future longitudinal studies should investigate how the identified differences in functional connectivity between smokers and nonsmokers change

with smoking cessation and relate to withdrawal, stress, and weight gain.

Conclusions

In summary, these data demonstrate group differences in functional connectivity in smokers and nonsmokers during exposure to personalized guided favorite-food, stress, and neutral-relaxing imagery. Favorite-food imagery exposure was associated with overall lower connectivity in the supramarginal gyrus in smokers than nonsmokers, but with greater connectivity between the supramarginal gyrus and motivation-reward brain regions. Neutral-relaxing imagery exposure was associated with greater connectivity in the precuneus and posterior insula/rolandic operculum in smokers than nonsmokers. Stress imagery was associated with lower connectivity in the cerebellum in smokers than nonsmokers. These findings suggest that smoking is associated with alterations in neural processing that may impact appetite, relaxation, and stress. These neural processes may represent targets for therapeutic interventions to support or promote smoking cessation, although this possibility warrants direct examination.

Supplementary Material

Supplementary Material can be found online at <http://www.ntr.oxfordjournals.org>

Funding

This work was funded by the National Institutes of Health through grants from the National Institute on Drug Abuse (K12DA00167, T32DA022975), National Institute on Alcohol Abuse and Alcoholism (RL1 AA017539), the NIH Common Fund grants UL1-DE019586, PL1-DA024859; CASA Columbia; and the American Heart Association (14CRP18200010).

Declaration of Interests

The authors declare no conflict of interest. MNP has consulted for Ironwood, Lundbeck, Shire, INSYS and RiverMend Health; has received research support from Mohegan Sun Casino, the National Center for Responsible Gaming, and Pfizer; has participated in surveys, mailings or telephone consultations related to drug addiction, impulse control disorders or other health topics; has consulted for legal and gambling entities on issues related to impulse control disorders; provides clinical care in the Connecticut Department of Mental Health and Addiction Services Problem Gambling Services Program; has performed grant reviews for the National Institutes of Health and other agencies; has edited/guest-edited journals or sections thereof; has given academic lectures in grand rounds, CME events and other clinical or scientific venues; and has generated books or book chapters for publishers of mental health texts.

Acknowledgments

We thank our research participants for their time and efforts. We thank Kwangik Adam Hong for his assistance with statistical analyses.

References

- Centers for Disease Control and Prevention. Quitting smoking among adults --- United States, 2001 -- 2010. *Morb Mortal Wkly Rep.* 2011;60(44):1513–1519. www.cdc.gov/mmwr/preview/mmwrhtml/mm6044a2.htm. Accessed September 1, 2015.
- Clinical Practice Guideline Treating Tobacco Use and Dependence 2008 Update Panel, Liaisons, and Staff. A clinical practice guideline for treating tobacco use and dependence: 2008 update. A U.S. Public Health Service report. *Am J Prev Med.* 2008;35(2):158–176. doi:10.1016/j.amepre.2008.04.009
- Engelmann JM, Versace F, Robinson JD, et al. Neural substrates of smoking cue reactivity: a meta-analysis of fMRI studies. *Neuroimage.* 2012;60(1):252–262. doi:10.1016/j.neuroimage.2011.12.024.
- Geha PY, Aschenbrenner K, Felsted J, O'Malley SS, Small DM. Altered hypothalamic response to food in smokers. *Am J Clin Nutr.* 2013;97(1):15–22. doi:10.3945/ajcn.112.043307.
- Tang DW, Fellows LK, Small DM, Dagher A. Food and drug cues activate similar brain regions: a meta-analysis of functional MRI studies. *Physiol Behav.* 2012;106(3):317–324. doi:10.1016/j.physbeh.2012.03.009.
- Jasinska AJ, Stein EA, Kaiser J, Naumer MJ, Yalachkov Y. Factors modulating neural reactivity to drug cues in addiction: a survey of human neuroimaging studies. *Neurosci Biobehav Rev.* 2014;38:1–16. doi:10.1016/j.neubiorev.2013.10.013.
- Sinha R. Chronic stress, drug use, and vulnerability to addiction. *Ann N Y Acad Sci.* 2008;1141:105–130. doi:10.1196/annals.1441.030.
- Jasinska AJ, Zorick T, Brody AL, Stein EA. Dual role of nicotine in addiction and cognition: a review of neuroimaging studies in humans. *Neuropharmacology.* 2014;84:111–122. doi:10.1016/j.neuropharm.2013.02.015.
- Lerman C, Gu H, Loughhead J, Ruparel K, Yang Y, Stein EA. Large-scale brain network coupling predicts acute nicotine abstinence effects on craving and cognitive function. *JAMA Psychiatry.* 2014;71(5):523–530. doi:10.1001/jamapsychiatry.2013.4091.
- Sutherland MT, McHugh MJ, Pariyadath V, Stein EA. Resting state functional connectivity in addiction: lessons learned and a road ahead. *Neuroimage.* 2012;62(4):2281–2295. doi:10.1016/j.neuroimage.2012.01.117.
- Jastreboff AM, Sinha R, Lacadie CM, Balodis IM, Sherwin R, Potenza MN. Blunted striatal responses to favorite-food cues in smokers. *Drug Alcohol Depend.* 2015;146:103–106. doi:10.1016/j.drugalcdep.2014.09.006.
- Sinha R, Talih M, Malison R, Cooney N, Anderson GM, Kreek MJ. Hypothalamic-pituitary-adrenal axis and sympatho-adreno-medullary responses during stress-induced and drug cue-induced cocaine craving states. *Psychopharmacology (Berl).* 2003;170(1):62–72. doi:10.1007/s00213-003-1525-8.
- Potenza MN, Hong KI, Lacadie CM, Fulbright RK, Tuit KL, Sinha R. Neural correlates of stress-induced and cue-induced drug craving: influences of sex and cocaine dependence. *A J Psychiatry.* 2012;169(4):406–414. doi:10.1176/appi.ajp.2011.11020289.
- McKee SA, Potenza MN, Kober H, et al. A translational investigation targeting stress-reactivity and prefrontal cognitive control with guanfacine for smoking cessation. *J Psychopharmacol.* 2015;29(3):300–311. doi:10.1177/0269881114562091.
- McKee SA, Sinha R, Weinberger AH, et al. Stress decreases the ability to resist smoking and potentiates smoking intensity and reward. *J Psychopharmacol.* 2011;25(4):490–502. doi:10.1177/0269881110376694.
- Jastreboff AM, Sinha R, Lacadie C, Small DM, Sherwin RS, Potenza MN. Neural correlates of stress- and food cue-induced food craving in obesity: association with insulin levels. *Diabetes Care.* 2013;36(2):394–402. doi:10.2337/dc12-1112.
- Lanius RA, Williamson PC, Hopper J, et al. Recall of emotional states in posttraumatic stress disorder: an fMRI investigation. *Biol Psychiatry.* 2003;53(3):204–210. doi:10.1016/S0006-3223(02)01466-X.
- Scheinost D, Benjamin J, Lacadie CM, et al. The intrinsic connectivity distribution: a novel contrast measure reflecting voxel level functional connectivity. *Neuroimage.* 2012;62(3):1510–1519. doi:10.1016/j.neuroimage.2012.05.073.
- Calhoun VD, Adali T, Pearlson GD, Pekar JJ. A method for making group inferences from functional MRI data using independent component analysis. *Hum Brain Mapp.* 2001;14(3):140–151.
- Huang W, King JA, Ursprung WW, et al. The development and expression of physical nicotine dependence corresponds to structural and functional

- alterations in the anterior cingulate-precuneus pathway. *Brain Behav.* 2014;4(3):408–417. doi:10.1002/brb3.227.
21. Clewett D, Luo S, Hsu E, Ainslie G, Mather M, Monterosso J. Increased functional coupling between the left fronto-parietal network and anterior insula predicts steeper delay discounting in smokers. *Hum Brain Mapp.* 2014;35(8):3774–3787. doi:10.1002/hbm.22436.
 22. Worhunsky PD, Stevens MC, Carroll KM, et al. Functional brain networks associated with cognitive control, cocaine dependence, and treatment outcome. *Psychol Addict Behav.* 2013;27(2):477–488. doi:10.1037/a0029092.
 23. Ray S, Gohel S, Biswal BB. Altered functional connectivity strength in abstinent chronic cocaine smokers compared to healthy controls. *Brain Connect.* 2015;5(8):476–486. doi:10.1089/brain.2014.0240.
 24. Garrison KA, Scheinost D, Constable RT, Brewer JA. BOLD signal and functional connectivity associated with loving kindness meditation. *Brain Behav.* 2014;4(3):337–347. doi:10.1002/brb3.219.
 25. Brewer JA, Worhunsky PD, Gray JR, Tang YY, Weber J, Kober H. Meditation experience is associated with differences in default mode network activity and connectivity. *Proc Natl Acad Sci USA.* 2011;108(50):20254–20259. doi:10.1073/pnas.1112029108.
 26. Mitchell MR, Balodis IM, Devito EE, et al. A preliminary investigation of Stroop-related intrinsic connectivity in cocaine dependence: associations with treatment outcomes. *Am J Drug Alcohol Abuse.* 2013;39(6):392–402. doi:10.3109/00952990.2013.841711.
 27. Finn ES, Shen X, Scheinost D, et al. Functional connectome fingerprinting: identifying individuals using patterns of brain connectivity. *Nat Neurosci.* 2015;18(11):1664–1671. doi:10.1038/nn.4135.
 28. Cole MW, Reynolds JR, Power JD, Repovs G, Anticevic A, Braver TS. Multi-task connectivity reveals flexible hubs for adaptive task control. *Nat Neurosci.* 2013;16(9):1348–1355. doi:10.1038/nn.3470.
 29. Heatherton TE, Kozlowski LT, Frecker RC, Fagerstrom KO. The Fagerstrom Test for Nicotine Dependence: a revision of the Fagerstrom Tolerance Questionnaire. *Br J Addict.* 1991;86(9):1119–1127. doi:10.1111/j.1360-0443.1991.tb01879.x.
 30. Robinson SM, Sobell LC, Sobell MB, Leo GI. Reliability of the Timeline Followback for cocaine, cannabis, and cigarette use. *Psychol Addict Behav.* 2014;28(1):154–162. doi:10.1037/a0030992.
 31. Sinha R. Modeling stress and drug craving in the laboratory: implications for addiction treatment development. *Addict Biol.* 2009;14(1):84–98. doi:10.1111/j.1369-1600.2008.00134.x.
 32. Jastreboff AM, Potenza MN, Lacadie C, Hong KA, Sherwin RS, Sinha R. Body mass index, metabolic factors, and striatal activation during stressful and neutral-relaxing states: an fMRI study. *Neuropsychopharmacology.* 2011;36(3):627–637. doi:10.1038/npp.2010.194.
 33. Friedman L, Glover GH, Krenz D, Magnotta V, Birn F. Reducing interscanner variability of activation in a multicenter fMRI study: role of smoothness equalization. *Neuroimage.* 2006;32(4):1656–1668. doi:10.1016/j.neuroimage.2006.03.062.
 34. Scheinost D, Papademetris X, Constable RT. The impact of image smoothness on intrinsic functional connectivity and head motion confounds. *Neuroimage.* 2014;95:13–21. doi:10.1016/j.neuroimage.2014.03.035.
 35. Joshi A, Scheinost D, Okuda H, et al. Unified framework for development, deployment and robust testing of neuroimaging algorithms. *Neuroinformatics.* 2011;9(1):69–84. doi:10.1007/s12021-010-9092-8.
 36. Scheinost D, Finn ES, Tokoglu F, et al. Sex differences in normal age trajectories of functional brain networks. *Hum Brain Mapp.* 2015;36(4):1524–1535. doi:10.1002/hbm.22720.
 37. Tomasi D, Volkow ND. Aging and functional brain networks. *Mol Psychiatry.* 2012;17(5):471, 549–458. doi:10.1038/mp.2011.81.
 38. Buckner RL, Sepulcre J, Talukdar T, et al. Cortical hubs revealed by intrinsic functional connectivity: mapping, assessment of stability, and relation to Alzheimer's disease. *J Neurosci.* 2009;29(6):1860–1873. doi:10.1523/JNEUROSCI.5062-08.2009.
 39. Anticevic A, Brumbaugh MS, Winkler AM, et al. Global prefrontal and fronto-amygdala dysconnectivity in bipolar I disorder with psychosis history. *Biol Psychiatry.* 2013;73(6):565–573. doi:10.1016/j.biopsych.2012.07.031.
 40. Tomasi D, Volkow ND. Gender differences in brain functional connectivity density. *Hum Brain Mapp.* 2012;33(4):849–860. doi:10.1002/hbm.21252.
 41. Cole MW, Pathak S, Schneider W. Identifying the brain's most globally connected regions. *Neuroimage.* 2010;49(4):3132–3148. doi:10.1016/j.neuroimage.2009.11.001.
 42. Tomasi D, Volkow ND. Abnormal functional connectivity in children with attention-deficit/hyperactivity disorder. *Biol Psychiatry.* 2012;71(5):443–450. doi:10.1016/j.biopsych.2011.11.003.
 43. Saad ZS, Gotts SJ, Murphy K, et al. Trouble at rest: how correlation patterns and group differences become distorted after global signal regression. *Brain Connect.* 2012;2(1):25–32. doi:10.1089/brain.2012.0080.
 44. Fox MD, Zhang D, Snyder AZ, Raichle ME. The global signal and observed anticorrelated resting state brain networks. *J Neurophysiol.* 2009;101(6):3270–3283. doi:10.1152/jn.90777.2008.
 45. Murphy K, Birn RM, Handwerker DA, Jones TB, Bandettini PA. The impact of global signal regression on resting state correlations: are anticorrelated networks introduced? *Neuroimage.* 2009;44(3):893–905. doi:10.1016/j.neuroimage.2008.09.036.
 46. Sutherland MT, Carroll AJ, Salmeron BJ, Ross TJ, Hong LE, Stein EA. Down-regulation of amygdala and insula functional circuits by varenicline and nicotine in abstinent cigarette smokers. *Biol Psychiatry.* 2013;74(7):538–546. doi:10.1016/j.biopsych.2013.01.035.
 47. Sutherland MT, Carroll AJ, Salmeron BJ, Ross TJ, Stein EA. Insula's functional connectivity with ventromedial prefrontal cortex mediates the impact of trait alexithymia on state tobacco craving. *Psychopharmacology (Berl).* 2013;228(1):143–155. doi:10.1007/s00213-013-3018-8.
 48. Janes AC, Nickerson LD, Frederick Bde B, Kaufman MJ. Prefrontal and limbic resting state brain network functional connectivity differs between nicotine-dependent smokers and non-smoking controls. *Drug Alcohol Depend.* 2012;125(3):252–259. doi:10.1016/j.drugalcdep.2012.02.020.
 49. Cole DM, Beckmann CF, Long CJ, Matthews PM, Durcan MJ, Beaver JD. Nicotine replacement in abstinent smokers improves cognitive withdrawal symptoms with modulation of resting brain network dynamics. *Neuroimage.* 2010;52(2):590–599. doi:10.1016/j.neuroimage.2010.04.251.
 50. Janes AC, Farmer S, Peechatka AL, Frederick Bde B, Lukas SE. Insula-dorsal anterior cingulate cortex coupling is associated with enhanced brain reactivity to smoking cues. *Neuropsychopharmacology.* 2015;40(7):1561–1568. doi:10.1038/npp.2015.9.
 51. Kaurijoki S, Kuikka JT, Niskanen E, et al. Association of serotonin transporter promoter regulatory region polymorphism and cerebral activity to visual presentation of food. *Clin Physiol Funct Imaging.* 2008;28(4):270–276. doi:10.1111/j.1475-097X.2008.00804.x.
 52. van Meer F, van der Laan LN, Adan RA, Vieregger MA, Smeets PA. What you see is what you eat: an ALE meta-analysis of the neural correlates of food viewing in children and adolescents. *Neuroimage.* 2015;104:35–43. doi:10.1016/j.neuroimage.2014.09.069.
 53. van der Laan LN, de Ridder DT, Vieregger MA, Smeets PA. The first taste is always with the eyes: a meta-analysis on the neural correlates of processing visual food cues. *Neuroimage.* 2011;55(1):296–303. doi:10.1016/j.neuroimage.2010.11.055.
 54. Yokum S, Stice E. Cognitive reappraisal strategies on neural response to palatable foods. *Int J Obes (Lond).* 2013;37(12):1565–1570. doi:10.1038/ijo.2013.39.
 55. Brody AL, Mandelkern MA, Olmstead RE, et al. Neural substrates of resisting craving during cigarette cue exposure. *Biol Psychiatry.* 2007;62(6):642–651. doi:10.1016/j.biopsych.2006.10.026.
 56. Russ MO, Mack W, Grama CR, Lanfermann H, Knopf M. Enactment effect in memory: evidence concerning the function of the supramarginal gyrus. *Exp Brain Res.* 2003;149(4):497–504. doi:10.1007/s00221-003-1398-4.
 57. Volkow ND, Fowler JS, Wang GJ, Swanson JM. Dopamine in drug abuse and addiction: results from imaging studies and treatment implications. *Mol Psychiatry.* 2004;9(6):557–569. doi:10.1038/sj.mp.4001507.

58. Chiolero A, Faeh D, Paccaud F, Cornuz J. Consequences of smoking for body weight, body fat distribution, and insulin resistance. *Am J Clin Nutr*. 2008;87(4):801–809.
59. Kroemer NB, Guevara A, Vollstadt-Klein S, Smolka MN. Nicotine alters food-cue reactivity via networks extending from the hypothalamus. *Neuropsychopharmacology*. 2013;38(11):2307–2314. doi:10.1038/npp.2013.133.
60. Mineur YS. Nicotine decreases food intake through activation of POMC neurons. *Science*. 2011;332(6035):1330–1332.
61. Cavanna AE, Trimble MR. The precuneus: a review of its functional anatomy and behavioural correlates. *Brain*. 2006;129(3):564–583. doi:10.1093/brain/awl004.
62. Zhang S, Li CS. Functional connectivity mapping of the human precuneus by resting state fMRI. *Neuroimage*. 2012;59(4):3548–3562. doi:10.1016/j.neuroimage.2011.11.023.
63. Buckner RL, Andrews-Hanna JR, Schacter DL. The brain's default network: anatomy, function, and relevance to disease. In: Kingstone A, Miller MB, eds. *The Year in Cognitive Neuroscience*. Malden, MA: Blackwell Publishing; 2008:1–38.
64. Raichle ME, MacLeod AM, Snyder AZ, Powers WJ, Gusnard DA, Gordon LS. A default mode of brain function. *Proc Natl Acad Sci USA*. 2001;98(2):676. doi:10.1073/pnas.98.2.676.
65. Fox MD, Snyder AZ, Vincent JL, Corbetta M, Van Essen DC, Raichle ME. The human brain is intrinsically organized into dynamic, anticorrelated functional networks. *Proc Natl Acad Sci USA*. 2005;102(27):9673–9678. doi:10.1073/pnas.0504136102.
66. Fox KC, Spreng RN, Ellamil M, Andrews-Hanna JR, Christoff K. The wandering brain: meta-analysis of functional neuroimaging studies of mind-wandering and related spontaneous thought processes. *Neuroimage*. 2015;111:611–621. doi:10.1016/j.neuroimage.2015.02.039.
67. Tang YY, Tang R, Posner MI. Brief meditation training induces smoking reduction. *Proc Natl Acad Sci USA*. 2013;110(34):13971–13975. doi:10.1073/pnas.1311887110.
68. Garrison KA, Pal P, Rojiani R, Dallery J, O'Malley SS, Brewer JA. A randomized controlled trial of smartphone-based mindfulness training for smoking cessation: a study protocol. *BMC Psychiatry*. 2015;15:83. doi:10.1186/s12888-015-0468-z.
69. Moran-Santa Maria MM, Hartwell KJ, Hanlon CA, et al. Right anterior insula connectivity is important for cue-induced craving in nicotine-dependent smokers. *Addict Biol*. 2014;20(2):407–414. doi:10.1111/adb.12124.
70. Stoodley CJ, Schmahmann JD. Evidence for topographic organization in the cerebellum of motor control versus cognitive and affective processing. *Cortex*. 2010;46(7):831–844. doi:10.1016/j.cortex.2009.11.008.
71. Moulton EA, Elman I, Becerra LR, Goldstein RZ, Borsook D. The cerebellum and addiction: insights gained from neuroimaging research. *Addict Biol*. 2014;19(3):317–331.
72. Miquel M, Toledo R, Garcia LI, Coria-Avila GA, Manzo J. Why should we keep the cerebellum in mind when thinking about addiction? *Curr Drug Abuse Rev*. 2009;2(1):26–40.
73. Claus ED, Blaine SK, Filbey FM, Mayer AR, Hutchison KE. Association between nicotine dependence severity, BOLD response to smoking cues, and functional connectivity. *Neuropsychopharmacology*. 2013;38(12):2363–2372. doi:10.1038/npp.2013.134.
74. Conklin CA, Perkins KA, Robin N, McClernon FJ, Salkeld RP. Bringing the real world into the laboratory: personal smoking and nonsmoking environments. *Drug Alcohol Depend*. 2010;111(1–2):58–63. doi:10.1016/j.drugalcdep.2010.03.017.
75. McClernon FJ, Conklin CA, Kozink RV, et al. Hippocampal and insular response to smoking-related environments: neuroimaging evidence for drug-context effects in nicotine dependence. *Neuropsychopharmacology*. 2015;41(3):877–885. doi:10.1038/npp.2015.214.
76. Carim-Todd L, Mitchell SH, Oken BS. Impulsivity and Stress Response in Nondependent Smokers (Tobacco Chippers) in Comparison to Heavy Smokers and Nonsmokers. *Nicotine Tob Res*. 2015:1–10. doi:10.1093/ntr/ntv210.
77. Kober H, Kross EF, Mischel W, Hart CL, Ochsner KN. Regulation of craving by cognitive strategies in cigarette smokers. *Drug Alcohol Depend*. 2010;106(1):52–55. doi:10.1016/j.drugalcdep.2009.07.017.
78. Rubinstein ML, Luks TL, Dryden WY, Rait MA, Simpson GV. Adolescent smokers show decreased brain responses to pleasurable food images compared with nonsmokers. *Nicotine Tob Res*. 2011;13(8):751–755. doi:10.1093/ntr/ntn046.
79. Rubinstein ML, Luks TL, Moscicki AB, Dryden W, Rait MA, Simpson GV. Smoking-related cue-induced brain activation in adolescent light smokers. *J Adolesc Health*. 2011;48(1):7–12. doi:10.1016/j.jadohealth.2010.09.016.
80. Poldrack RA. Can cognitive processes be inferred from neuroimaging data? *Trends Cogn Sci*. 2006;10(2):59–63.
81. Hutzler F. Reverse inference is not a fallacy per se: cognitive processes can be inferred from functional imaging data. *Neuroimage*. 2014;84:1061–1069. doi:10.1016/j.neuroimage.2012.12.075.